

Theoretical investigation of random Si-C alloys

Alexander A. Demkov and Otto F. Sankey

Department of Physics and Astronomy, Arizona State University, Tempe, Arizona 85287

(Received 7 December 1992)

We have performed a first-principles investigation of the microscopic properties of random crystalline Si-C alloys. An *ab initio* tight-binding molecular-dynamics method is used to determine the microscopic atomic structure of the alloys. For small to moderate concentrations of C in Si, we find that the electronic structure shows a decrease of the band gap from that of pure Si. This result is unexpected since both ordered SiC and pure carbon (diamond) have much larger band gaps than Si. Plane-wave calculations were also done on ordered structures to further check this result and to determine the effects of ordering. For the atomic structure, it is found that there are two different types of Si-C bonds. The first type is the Si-C bond near 1.86 Å as in bulk SiC, and the second type is a much shorter 1.65-Å bond for a carbon atom in a near-planar sp^2 configuration with its Si neighbors.

I. INTRODUCTION

The significant success of semiconductor electronics is closely connected to the concept of band-gap engineering. The band gap of a semiconductor can be significantly altered by alloying, and this is routinely done in III-V semiconductor materials, such as $Al_xGa_{1-x}As$. In the Si-based materials, the band gap has been successfully altered by alloying with Ge and by forming strained layer superlattices.¹ Low concentrations of Ge in $Si_{1-x}Ge_x$ alloys provide a family of band structures similar to that of Si, with the indirect gap near the X point of the Brillouin zone. The band gap, however, decreases monotonically as the Ge concentration increases. The entire band gap range for $Si_{1-x}Ge_x$ alloys varies between 1.17 eV ($x=0$) and 0.62 eV ($x=1$). In many applications it is desirable to have a band gap which is wider than that of pure Si. Diamond with its very wide band gap of 5.5 eV is a possible candidate for making a wide band-gap Si-based material which can be integrated with Si. However, diamond has a much smaller lattice parameter than Si, which makes the structural aspects of the Si-C alloy system quite unlike those of $Al_xGa_{1-x}As$ or $Si_{1-x}Ge_x$ alloys.

The main obstacle to the realization of this program is the extremely low solubility of C in Si. Even at the melting point of Si, it is only about 10^{-6} at. %.² This problem has been partially overcome recently. The first successful attempt to grow $Si_{1-x}C_x$ alloys was reported by Posthill *et al.*³ Using remote plasma-enhanced chemical-vapor deposition this group fabricated a 7- μ m-thick layer with a carbon concentration of about 3.5%. The lattice parameter perpendicular to the substrate was found to be 5.426 Å. At this concentration, if all the carbon goes substitutionally and the film is grown on Si, the lattice parameter perpendicular to the substrate should range from 5.37 (fully relaxed) to 5.24 Å (fully strained). The observed lattice parameter indicates that there may be some precipitation of SiC in the film or that this material does not obey Vegard's rule. This work was followed by the

work of Iyer *et al.*² who used solid source molecular-beam epitaxy to grow pseudomorphic $Si_{1-x}C_x$ layers with $x > 0.002$ and strained layered superlattices stable up to 800° (for $x=0.003$). Their material also contained about 1% Ge to compensate for strain effects.

The band gaps of $Si_{1-x}C_x$ alloys and related alloys have recently been theoretically investigated by Soref⁴ using an interpolation technique. Indeed, he predicts that the band gap of Si increases dramatically upon alloying with C. The band gap of the ordered SiC compound, which has a band gap of 2.39 eV, is predicted to be close to that of the $Si_{0.5}C_{0.5}$ random alloy. We are unaware of any first-principles calculations of the electronic structure of these alloys. This is partially attributed to the relative complexity of the first-principles calculation involving carbon and its compounds. Recently, several theoretical studies of SiC have been reported. The ground-state properties (equilibrium lattice constant and bulk modulus) have been calculated by Denteneer and van Haeringen.⁵ Churcher, Kunc, and Heine⁶ also calculated the pressure derivative of the bulk modulus and the Gruneisen parameters. High-pressure properties of SiC were discussed by Chang and Cohen.⁷ Wang, Bernholc, and Davis calculated formation energies, abundances, and the electronic structure of native defects in cubic SiC.⁸ All this work has utilized the local density approximation within the density-functional theory and the pseudopotential method. Calculations of the properties for the related material, GeC, have just recently been performed.⁹

The microscopic structure of the equimolar Si-C amorphous alloy has been studied by Finocchi *et al.*¹⁰ with *ab initio* molecular dynamics. These authors find that the system cannot be classified as chemically ordered since 40–50% of the bonds are homonuclear, nor can it be classified as random since a high degree of short- to medium-range order exists. They also find the electronic density of states is semiconductorlike, but is certainly much smaller than the 2.39-eV experimental gap of ordered crystalline SiC.

In this paper we have studied the electronic and geometrical atomic structure of Si-C random alloys. We have used *ab initio* tight-binding-like molecular dynamics to obtain the geometrically relaxed atomic structure of random 64-atom supercells for five $\text{Si}_{1-x}\text{C}_x$ alloys with carbon concentrations (x) of 1.6, 6.2, 10.9, 25, and 50%. We also obtained the electronic structure of these alloys. In addition, we have also studied smaller 8-atom ordered cells using a pseudopotential plane-wave method to determine the effects of ordering, lattice relaxation, and basis set. It is found that there is a large lattice relaxation around the carbon atoms. We also find that the most typical Si-C bond in our simulation is 1.86 Å which is close to the corresponding bond in the zinc-blende SiC. However, we also find another much shorter Si-C bond of 1.65 Å. The carbon atom has a strong chemical effect on the band structure which causes the band gap of Si to sharply drop, and possibly become metallic at a concentration of about 5–10%. This effect is not driven by the geometrical relaxation or ordering, but by the atomic properties of carbon itself.

The rest of the paper is organized as follows. A brief theoretical background of the methods used in this study is given in Sec. II. In Sec. III we describe results obtained for the microscopic atomic arrangement of five Si-C alloys in 64-atom cubic supercells. In Sec. IV we describe our results for the electronic structure. Discussion and conclusions are found in Sec. V.

II. THEORETICAL BACKGROUND

We addressed two basic questions in this study of Si-C alloys: (i) the local atomic geometry of the alloy, and (ii) its electronic structure. Of particular interest here is the basic trend in these as small amounts of carbon are added to silicon.

To deal with the first of these questions we have chosen the *ab initio* simplified tight-binding-like quantum molecular-dynamics (QMD) method of Sankey and Niklewski.¹¹ In this method the total energy of the system is calculated using localized slightly excited atomic orbitals (fireballs) in the local density approximation and the pseudopotential approximation. The forces acting on every atom are determined using a variation of the Hellman-Feynman theorem.^{12,13} Given the forces at any configuration, atoms are geometrically relaxed by allowing them to move according to Newton's laws in the presence of a fictitious damping force. The system evolves until an equilibrium (zero force) geometry is obtained and the final atomic configuration is established.

We have used this technique to geometrically relax 64-atom cells, and in addition obtain the electronic structure of these cells. We start with atomic sites of perfect tetrahedral symmetry in the zinc-blende lattice. The 64-atom cell contains 8 cubes of the zinc-blende lattice of lattice constant $a(x)$. We use Vegard's rule to determine the lattice constant, $a(x) = (1-x)a_{\text{Si}} + xa_{\text{C}}$, where a_{Si} and a_{C} are the cubic lattice constants of Si (5.43 Å) and C (3.57 Å), respectively. A random number generator is used to choose whether a site is occupied by Si or C at a specific concentration. The system is then geometrically

relaxed, and may form a highly distorted structure.

To check our results for the band structure, and to determine the effect of ordering we have also performed plane-wave pseudopotential calculation for a single 8-atom cubic cell. These were done using the non-self-consistent Harris approximation.¹⁴ One fully self-consistent calculation was done to check that the Harris approximation was giving the correct results. Due to the strong p pseudopotential of carbon, we have used the soft pseudopotentials of Kerker, and Trouillier and Martins.¹⁵ The number of plane waves used in these calculations was determined by an energy cutoff of 500 eV.

III. ATOMIC MICROSTRUCTURE

The microscopic structure of the Si-C alloys was obtained using QMD. A 64-atom simple cubic unit cell was used, with sites randomly occupied by Si and C atoms of a given concentration. The size of the cell was chosen according to Vegard's rule. We quenched the structure by molecular dynamics until the zero force configuration was found. Only the Γ point was used for the sampling of the supercell Brillouin zone in all simulations except the one for the 10.9% alloy where we used eight special k points over entire zone. Studies of the convergence of the force versus k -point sampling in amorphous Si supercells have been performed¹⁶ using the present method, and for the 64-atom supercells used here, the use of the Γ point is an acceptable approximation and is used here.

Let us begin with a single carbon atom in the 64-atom supercell, which gives a carbon concentration of 1.6%. The radial distribution functions (RDF) for the relaxed structure are shown in Fig. 1. The radial distribution function $g_{AB}(r)$ represents the probability to find an atom of type B at the distance r from the atom of type A . We replace the δ -function peaks by Gaussians of width of 0.025 Å. The first peak in the C-Si RDF at 1.86 Å can be compared with the SiC nearest-neighbor (NN) distance of 1.89 Å. Similarly, the second peak of $g_{\text{C Si}}$ at 3.7 Å lies between the second-NN distance of bulk Si (3.84 Å) and of zinc-blende SiC (3.08 Å). In the Si-Si RDF, we observe the intense first peak at 2.33 Å (compare to 2.35 Å in

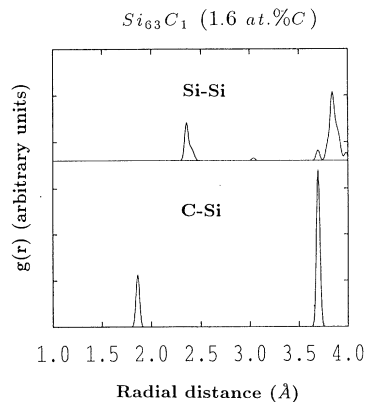


FIG. 1. Computed radial distribution functions g_{AB} ($A, B = \text{C, Si}$) for the 64-atom supercell Si_{63}C_1 . The δ -function peaks are replaced by Gaussians of width of 0.025 Å.

pure Si). One can also see a shoulder at approximately 2.42 Å. The first-NN Si atoms have moved in by 0.49 Å along (111) directions and the second NN moved in by 0.144 Å along (110) directions compared to their ideal diamond lattice positions. We conclude that large lattice relaxation occurs around the C atom. From this analysis we conclude that at very low concentration of C in Si, C atoms recreate a SiC environment around them.

In order to test how well our method describes the actual structural relaxation, we have done the following model calculation. We have studied the first-nearest-neighbor relaxation around a single substitutional carbon atom in an 8-atom silicon cubic cell. Only the first-nearest-neighbor Si atoms around carbon were allowed to move along (111) directions and the displacements were measured from their ideal position in pure Si. The total energy per cell as a function of displacement is shown in Fig. 2. Three different methods were used in this calculation: our QMD technique, a plane-wave technique within the Harris approximation (Harris PW), and a standard self-consistent plane-wave method (SCPW). All three computational techniques give very similar results for the energy lowering and the amount of near-neighbor relaxation. The equilibrium positions differ in a few hundredths of an angstrom and the energy spread is about 0.2 eV. The Harris approximation seems to be more important than the choice of the basis set: the two calculations using this approximation give almost identical results. We conclude that our molecular-dynamics method gives an accurate description of the microscopic structure for the Si-C system. It is perhaps worth mentioning that the 8-atom cell does not give the same equilibrium position of Si atoms which are C nearest neighbors as the 64-

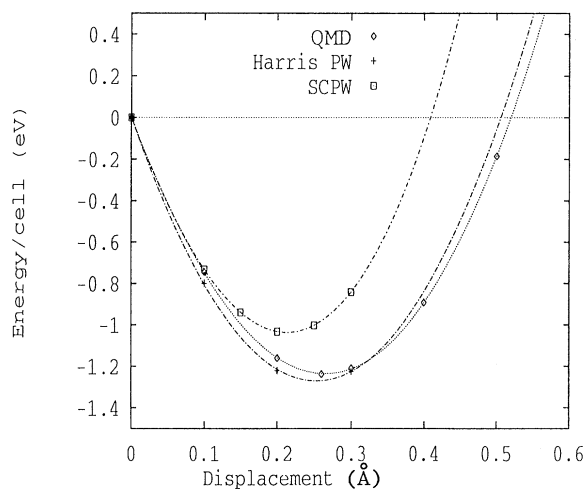


FIG. 2. Energy per cell vs displacement of carbon atom first neighbors for the 8-atom cell Si_7C_1 calculated by three different methods: the tight-binding-like quantum molecular dynamics, the plane-wave method using the Harris energy functional (labeled Harris PW), and the standard plane-wave self-consistent technique (labeled SCPW). Only first neighbors were allowed to move. The energy of zero corresponds to the zero displacement. The lattice constant was taken to be that of bulk Si.

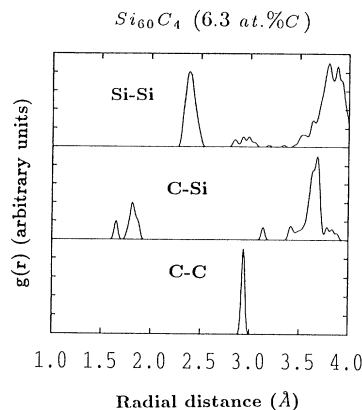


FIG. 3. Computed radial distribution functions for the 64-atom supercell Si_{60}C_4 g_{AB} , $A, B = \text{C, Si}$. The δ -function peaks are replaced by Gaussians of width of 0.025 Å.

atom cell because the second-nearest neighbors have not been allowed to move in the 8-atom cell calculation.

Now let us examine the structure of the 6.3% alloy which contains four C atoms and 60 Si atoms. As we can see from the C-C RDF in Fig. 3 there are no C-C bonds in this randomly generated sample. The first peak occurs at about 2.9 Å and clearly corresponds to the second-nearest-neighbor distance intermediate between a bulk C second-nearest-neighbor distance of 2.52 Å and a bulk Si second-nearest-neighbor distance of 3.84 Å. The most interesting structure in this sample is revealed by the C-Si RDF. We find a prominent peak at 1.88 Å with a small

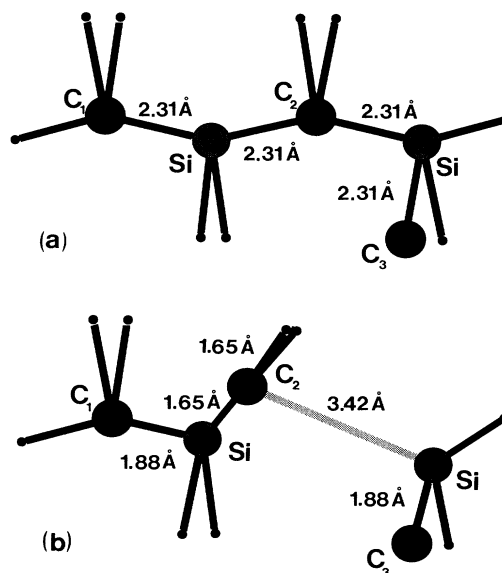


FIG. 4. A schematic picture of a fragment of the structure of a 6.3% C concentration in Si (Si_{60}C_4 supercell). Three of the four carbon atoms in the supercell were randomly selected to be second neighbors of each other. (a) The local geometry before relaxation of the atomic coordinates. (b) The zero force final configuration of the fragment. Notice formation of a CSi_3 graphitic structure with the atom C_2 in the center.

shoulder at a larger distance. The prominent peak corresponds closely to the single carbon surrounded by perfect silicon tetrahedral configuration found in the single carbon sample.

A new feature of the C-Si RDF is a peak at 1.65 Å. To understand its nature we must examine the actual configuration in the sample. A fragment of the structure relevant to the 1.65-Å peak is schematically reproduced in Fig. 4. In Fig. 4(a) we show the initial (nonrelaxed)

tetrahedral configuration. By chance, three carbon atoms happened to be second-nearest neighbors of each other. The atoms are allowed to relax according to their forces and each carbon atom tries to form SiC tetrahedrons around it. The average bond length of 2.13 Å is far from that of the SiC bond length of 1.89 Å. Not all three carbon atoms can successfully form the SiC tetrahedron. The two shown silicon atoms surrounding C_2 cannot get close to both its neighboring carbon atoms, so C_2 must sacrifice one of its bonds with Si. The carbon atom C_2 moves along a (111) direction where it finds itself in a nearly flat triple coordination very much like the one in graphite [see Fig. 4(b)]. This “graphitic” SiC bond is found to be 1.65 Å, considerably shorter than the zincblende tetrahedral SiC bond length. The final relaxed configuration is somewhat close to that proposed for the EL2 defect in GaAs (sp^2 coordinated As interstitial and Ga vacancy).¹⁷

The radial distribution function for the 10.9% alloy is shown in Fig. 5(a). The C-C RDF still has no C-C bonds, but we see a peak at 2.75 Å and a family of peaks in the range from 3.2 to 3.5 Å (the second-nearest-neighbor distance is 2.52 Å in diamond, 3.18 Å in SiC, and 3.65 Å according to Vegard’s rule for this concentration). In the C-Si RDF we see two groups of peaks corresponding to two different kinds of nearest neighbors. One group is centered near 1.9 Å which is typical for the tetrahedral SiC-type configuration, and another group is centered about 1.65 Å suggesting the sp^2 configuration of carbon, similar to one discussed in the previous example. In the Si-Si RDF, we find a prominent peak at 2.35 Å and a whole family of peaks in the second-nearest-neighbor region. The feature of this RDF is the presence of “noise” between the first- and second-nearest-neighbor peaks.

In the 25% and 50% carbon alloys, the radial distribution functions become quite complex [Figs. 5(b) and 5(c)]. We see C-C bonds starting near 1.5 Å. In the 50% alloy [Fig. 5(c)] there is a small peak in the C-C RDF at 1.4 Å (compare with 1.42 Å in graphite) and a prominent peak at 1.55 Å (compare with 1.55 Å in diamond). In the C-Si RDF’s, we can see that the “tetrahedral” peak at 1.89 Å has decreased, while the peak at 1.65 Å has increased. This suggests the disintegration of the tetrahedral network similar to one found in amorphous Si-C alloys.¹⁰

IV. ELECTRONIC STRUCTURE

The electronic structure of random semiconductor alloys is commonly described in terms of a mean-field or “virtual crystal” theory in which each atom is replaced by an average atom and the electronic properties are interpreted in terms of a perfect crystal of these average atoms. Such a description leads to a near linear dependence of the band gap with composition, but also predicts some bowing of the band edges to occur. For example, such a description well describes the band gaps of $Si_{1-x}Ge_x$ random alloys.^{18,19} We now show that such a mean-field picture is totally inappropriate for $Si_{1-x}C_x$ alloys—the band gaps that we find cannot be understood as being generated by an average atom, and that interpolation of the band gap for the alloy from pure crystalline

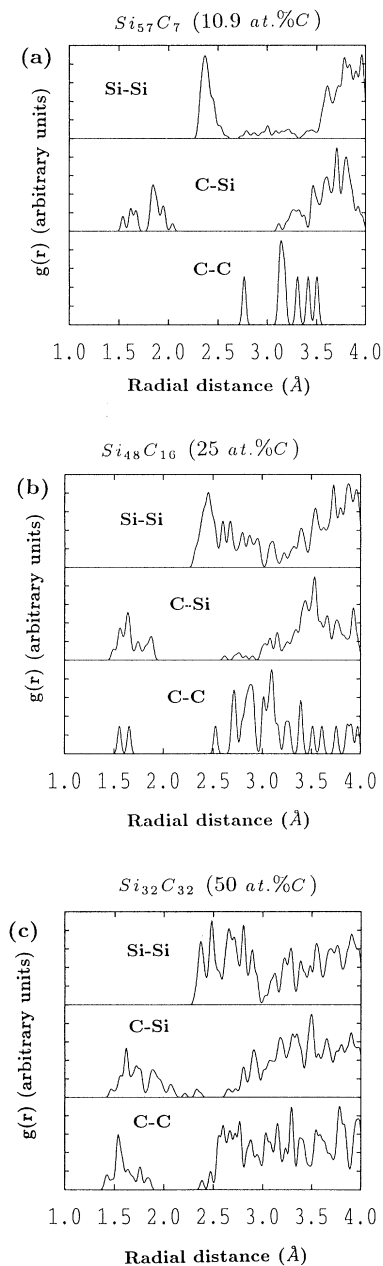


FIG. 5. (a) Computed radial distribution functions for the 64-atom supercell $Si_{57}C_7$. (b) Computed radial distribution functions for the 64-atom supercell $Si_{48}C_{16}$. (c) Computed radial distribution functions for the 64-atom supercell $Si_{32}C_{32}$. The δ -function peaks are replaced by Gaussians of width of 0.025 Å.

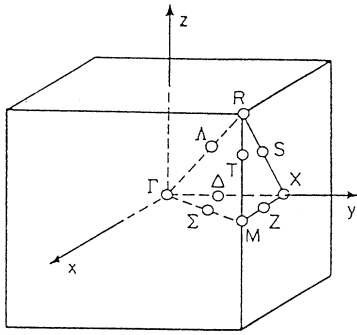


FIG. 6. The first Brillouin zone of the simple cubic lattice.

Si to pure carbon diamond gives qualitatively incorrect results.

We have studied the electronic structure of the random Si-C alloy structures in supercells containing 64 atoms with an average bond length determined by Vegard's law. The QMD relaxation procedure determines the atomic configuration of the cell as was described in Sec. III. Since the 64-atom cell is cubic, the first Brillouin zone is cubic and is shown in Fig. 6.

The band structure of pure silicon in a 64-atom cell is shown in Fig. 7(a). The top of the valence band is defined to have energy equal to zero, and the main band gap in this sp^3 -orbital model is 1.75 eV. The conduction-band minimum is along the line Γ to X in the supercell, as it is in the 2-atom primitive Brillouin zone. The band gap is larger than the experimental band gap of 1.17 eV due to the fact that we use a localized orbital sp^3 basis. The sp^3 basis is a minimal basis, which gives its largest error in

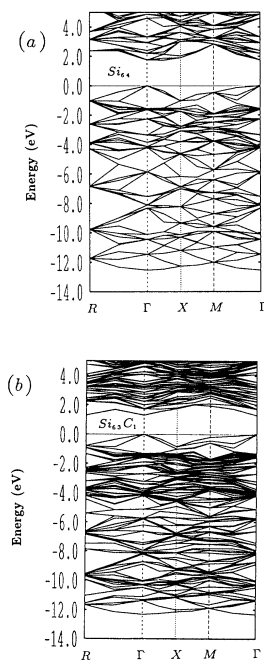


FIG. 7. The electronic structure for the 64-atom cell computed using our sp^3 -orbital model. (a) Pure silicon Si_{64} . (b) $Si_{0.984}C_{0.016}$ alloy $Si_{63}C_1$, geometrically relaxed by QMD.

the conduction bands. The bands of Si are opened by about 1 eV compared to the exact local-density-approximation results, with the major effect being due to the lack of d states.²⁰ Since we are interested in how the gap changes with alloy composition, this adds some uncertainty to the results. The trends with alloy composition ought to be adequately described, however. The trends we obtain with this basis are in fact well reproduced by the plane-wave calculations discussed later, which do not suffer from this restriction.

We next substitute a C atom for a Si atom in the 64-atom cell giving an effective concentration of carbon of 1.6%. The band structure of this system after geometrical relaxation is shown in Fig. 7(b). Note that the lowest conduction bands have dropped down to a lower energy reducing the band gap to 1.3 eV at both the Γ and the R points of the Brillouin zone. Thus the effect of a single substitutional carbon atom in a 64-atom Si supercell is to form a state near the perfect Si conduction-band minimum which tends to lower the gap. This is very similar to the behavior expected for a single substitutional impurity in bulk Si, which theoretically is expected to form a "deep level" almost degenerate with the conduction-band edge.²¹

We show the lowest conduction-band eigenenergies at the Γ (000), X (100), and R (111) Brillouin-zone points for relaxed random alloys of 0.0, 1.6, 6.3, 10.9, and 25% carbon. The valence-band maximum is always at $k = (0,0,0)$ and is defined to have energy zero. The results are shown in Fig. 8. The trend that the band decreases for small carbon concentration is evident at each Brillouin-zone point. The system reaches a minimum band gap near 12.5%, and in fact is predicted to be metallic. To put this result in perspective, the same sp^3 -orbital-based model predicts the minimum band gap of perfect crystalline Si, SiC, and C to be 1.75, 4.3, and 5.9 eV. Thus it is quite

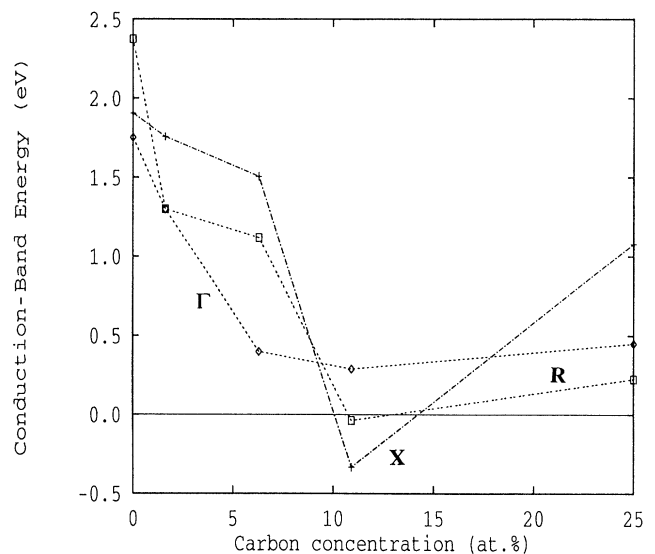


FIG. 8. Conduction-band eigenenergies at the Γ , R , and X points of the Brillouin zone vs carbon concentration computed for 64-atom cells geometrically relaxed by QMD.

evident that band-gap behavior for the random alloy shown in Fig. 8 is quite unlike a mean-field result.

The band gaps that we find for the 64-atom unit cell are a result of both the chemistry of the Si-C system and the distorted geometries and strains we obtain in the random alloy. To investigate the effect of strain and the possible role of ordering within the alloys, we have performed similar calculations on a much smaller cell of 8 atoms. Such a cell is small enough that ordering effects will be greatly enhanced. The band structure of pure silicon in an 8-atom cell is shown in Fig. 9(a). The main energy gap lies along Γ to X and is again 1.75 eV as it must be. When a single C atom is substituted for Si we obtain an ordered cell with an effective concentration of 12.5%. The lattice parameter for this cell was varied according to Vegard's rule. The band structures obtained for this Si_7C_1 cell are shown in Figs. 9(b) and 9(c). In Fig. 9(b) we keep the atoms at their perfect tetrahedral (unrelaxed) positions, while in Fig. 9(c) we show the band structure

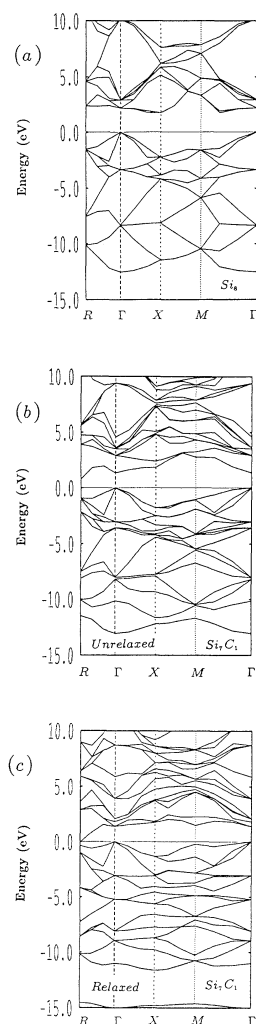


FIG. 9. The electronic structure for the 8-atom cell computed using our sp^3 -orbital model. (a) Pure silicon Si_8 . (b) $\text{Si}_{0.875}\text{C}_{0.125}$ alloy Si_7C_1 in the perfect tetrahedral geometry. (c) The same alloy as in (b) but geometrically relaxed by QMD.

obtained when the atoms are allowed to relax (using QMD) to their equilibrium positions. In either case (unrelaxed or relaxed) we see that the band gap has been greatly reduced compared to pure Si [Fig. 9(a)]. In this example, the effect of the relaxation of the Si toward the C to form a SiC-like bond is to further shrink the gap. The most sensitive band edge to relaxation is seen to be the R (111) k point. The relaxed structure in fact turns out to be a semimetal.

Comparing Figs. 9(b) and 9(c) shows that the effect of relaxation also has an important effect deep in the valence band. As the Si atoms move toward C, they strengthen their bonds and the “hyper-deep” carbonlike level near 14–15 eV has peeled further away from the rest of the valence band.

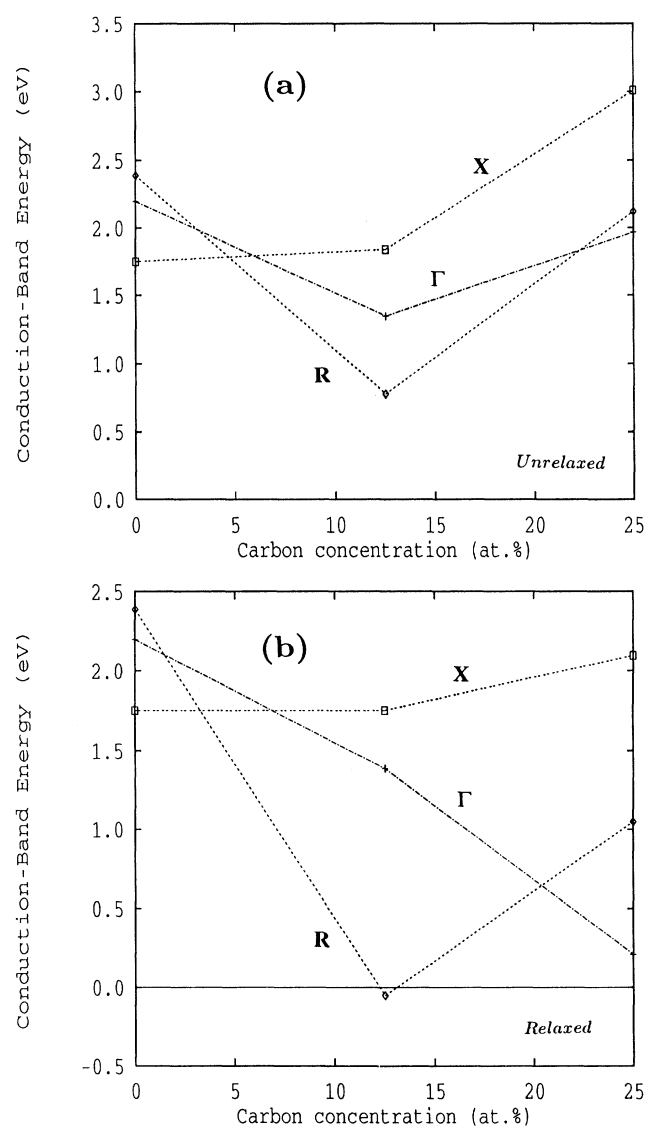


FIG. 10. Conduction-band eigenenergies at the Γ , R , and X points of the Brillouin zone vs carbon concentration computed for 8-atom cells using our sp^3 -orbital model. (a) Perfect tetrahedral geometry. (b) After being geometrically relaxed by QMD.

We have repeated these 8-atom cell calculations for two carbon atoms (25% carbon). We choose to put the two carbon atoms so that they are second neighbors. The conduction-band levels at Γ , X , and R at 0.0, 12.5, and 25% carbon concentration in the 8-atom cells which are perfectly tetrahedral (labeled unreaxed) or QMD relaxed (labeled relaxed) are shown in Figs. 10(a) and 10(b), respectively. Again we see that the band gap for all carbon concentrations is reduced compared to pure Si. The band gap is large for 25% C in the unreaxed 8-atom cell, but relaxation of the atoms again causes the band gap to be reduced.

From these 8-atom calculations we make two important conclusions. The first is that the band-gap shrinkage as carbon is added to Si is not just due to the randomness of the alloy system, but occurs even for small ordered cells such as Si_7C_1 and Si_6C_2 . The second conclusion is that the effect of lattice relaxation from all equal bond

lengths and perfectly tetrahedral bonds in these small cells is to further reduce the gap, and not to open it up again. Thus shrinkage of the Si band gap as carbon is added is a result of the large chemical difference between carbon and Si and not a geometrical effect.

As a final test of our conclusion that a small concentration of carbon in silicon reduces the Si band gap, we have performed plane-wave pseudopotential calculations on small 8-atom cubic cells for 0, 12.5, 25, 50, 75, and 100% carbon concentrations. The pseudopotentials are of the Troullier and Martins form⁵ and we use the energy cutoff of 300 eV for Si and 500 eV for the alloys and diamond. We have used the approximate Harris local density energy functional,¹⁴ which does not require self-consistency. We have repeated the calculations using the standard self-consistent local-density-approximation energy functional for 12.5% carbon and find no significant change in the trends. For pure Si we obtain an energy gap of 1.05 eV (experimental, 1.17 eV), and for pure C an energy gap of 4.88 eV (experimental, 5.5 eV).

The band structures for the 8-atom cells using plane waves for 0% and 12.5% C are shown in Figs. 11(a), 11(b), and 11(c). Figure 11(a) is for pure Si in an 8-atom cell (Si_8) while Figs. 11(b) and 11(c) are for one carbon atom in an 8-atom cell (Si_7C_1). Again we see that the band gap has closed in Si_7C_1 compared to that for Si_8 . The effect of lattice relaxation is indicated by comparing Figs. 11(b) and 11(c) which correspond to unreaxed and relaxed structures, respectively. The relaxed coordinates are those obtained using our *sp*-orbital-based QMD technique and are the same coordinates as were used to create Fig. 9(c). Relaxation of the atoms toward their zero force bond lengths and angles further reduces the band gap in agreement with the previous calculations. Again, as in the *sp*³ QMD technique, 12.5% C is found to be metallic.

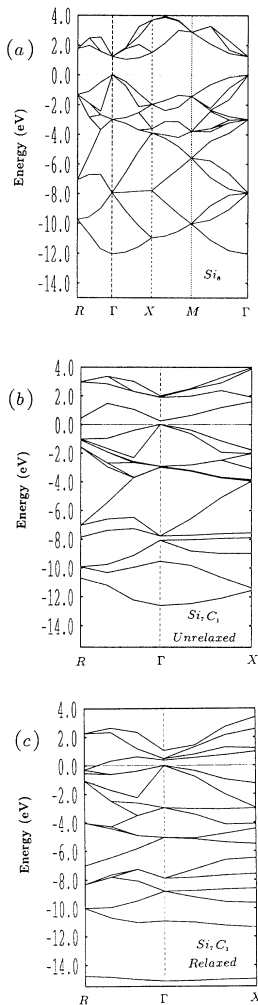


FIG. 11. The electronic structure for the 8-atom cell computed using the plane-wave method and the Harris energy functional. (a) Pure silicon Si_8 . (b) $\text{Si}_{0.875}\text{C}_{0.125}$ alloy Si_7C_1 in the perfect tetrahedral geometry. (c) The same alloy as in (b) relaxed by QMD.

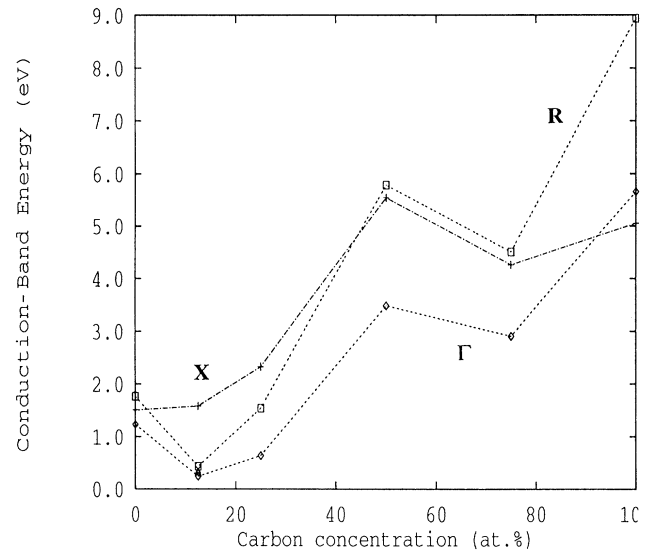


FIG. 12. Conduction-band eigenenergies at the Γ , R , and X points of the Brillouin zone vs carbon concentration computed for 8-atom cells using the plane-wave method and the Harris energy functional. All cells are unreaxed (perfect tetrahedral bonding) with a lattice constant determined by Vegard's rule.

The conduction-band edges at Γ , X , and R for the 8-atom cell computed using plane waves are shown in Fig. 12. To produce this figure, we have arranged the atoms so that minority atoms are never nearest neighbors, and the geometry is an ideal zinc-blende lattice (i.e., no relaxation). We find an unusual "double well" shape for the minimum band gap versus composition. The band gap apparently gets smaller for both larger and smaller carbon concentrations away from that of bulk zinc-blende SiC (i.e., 50% carbon).

V. CONCLUSION

We have presented results from an *ab initio* study of the random crystalline $\text{Si}_{1-x}\text{C}_x$ alloys. We have used a simplified first-principles molecular-dynamics method to investigate the atomic structure of the alloys using 64-atom cubic supercells with an average bond length scaled according to Vegard's rule. Ideal cells were geometrically relaxed to the minimum energy configuration, and atomic radial distribution functions were obtained for the relaxed geometry. It is found that the random alloy forms a minimum energy geometry in which silicon nearest-neighbor bonds are close to those of pure Si, and Si-C bonds are close to those of bulk SiC. Carbon-carbon bonds are found representing both diamond and graphite types bonds. We also find for larger carbon concentrations the appearance of CSi_3 planar (graphiticlike) struc-

tures of bond length of about 0.2 Å less than that of the tetrahedral SiC bond length.

Concerning the electronic structure, it is found that for small concentrations of carbon in Si, the band gap shrinks compared to that of pure Si. The gap reaches a minimum value which is likely negative (a metal) around 10% carbon. The origin of this effect is due to the large chemistry difference of carbon compared to Si. Lattice distortion of the alloy compared to a perfect tetrahedral zinc-blende-like lattice tends to make the minimum gap even smaller. Randomness is also not a dominant factor in the result that the Si band gap closes as carbon is added, since the same effect occurs with small ordered 8-atom cubic cells. The alloy dependence of the band gap of $\text{Si}_{1-x}\text{C}_x$ alloys is quite unlike that of $\text{Si}_{1-x}\text{Ge}_x$ alloys and for that matter all other semiconductor systems. We hope these results will stimulate experimental interest in this unexplored, but probably metastable, material.

ACKNOWLEDGMENTS

We wish to thank the Office of Naval Research for its support under Grant No. ONR-N00014-90-J-1304, and the NSF materials research group Grant No. DMR 91-21570. We appreciate stimulating conversations with Dr. José Ortega, James Lewis, Professor Jim Mayer, Professor William Petusky, Professor Paul McMillan, and Professor Nicole Herbots.

-
- ¹S. S. Iyer, G. L. Patton, J. M. C. Stork, B. S. Meyerson, and D. L. Harnam, *IEEE Trans. Electron. Devices* **ED-36**, 2043 (1989).
- ²S. S. Iyer, K. Eberl, M. S. Gorsky, F. K. Legoues, F. Cardone, and B. A. Ek, in *Silicon Molecular Beam Epitaxy*, edited by J. C. Bean, S. Iyer, and K. Wang, MRS Symposia Proceedings No. 220 (Materials Research Society, Pittsburgh, 1991), p. 581.
- ³J. B. Posthil, R. A. Rudder, S. V. Hattangady, G. G. Fountain, and R. J. Markunas, *Appl. Phys. Lett.* **56**, 734 (1990).
- ⁴R. A. Soref, *J. Appl. Phys.* **70**, 2470 (1991).
- ⁵P. J. H. Denteneer and W. van Haeringen, *Phys. Rev. B* **33**, 2831 (1986).
- ⁶N. Churcher, K. Kunc, and V. Heine, *J. Phys. C* **19**, 4413 (1986).
- ⁷K. J. Chang and M. L. Cohen, *Phys. Rev. B* **35**, 8196 (1987).
- ⁸C. Wang, J. Bernholc, and R. F. Davis, *Phys. Rev. B* **38**, 12 752 (1988).
- ⁹O. F. Sankey, A. A. Demkov, W. T. Petusky, and P. F. McMillan, *Modell. Simulat. Mater. Sci. Eng.* (to be published).
- ¹⁰F. Finocchi, G. Galli, M. Parrinello, and C. M. Bertoni, *Phys. Rev. Lett.* **68**, 3044 (1992).
- ¹¹O. F. Sankey and D. J. Niklewski, *Phys. Rev. B* **40**, 3979 (1989).
- ¹²H. Hellmann, *Einführung in die Quantumchemie* (Franz Deutsche, Leipzig, 1937).
- ¹³R. P. Feynman, *Phys. Rev.* **56**, 340 (1939).
- ¹⁴J. Harris, *Phys. Rev. B* **31**, 1770 (1985).
- ¹⁵G. Kerker, *J. Phys. C* **13**, 189 (1980); M. Troullier and J. L. Martins, *Phys. Rev. B* **43**, 1993 (1991).
- ¹⁶D. A. Drabold, J. D. Dow, P. A. Fedders, A. E. Carlsson, and O. F. Sankey, *Phys. Rev. B* **42**, 5345 (1990).
- ¹⁷J. Dabrowsky and M. Scheffler, *Phys. Rev. Lett.* **60**, 2183 (1988).
- ¹⁸K. E. Newman and J. D. Dow, *Phys. Rev. B* **30**, 1929 (1984).
- ¹⁹S.-F. Ren, K. E. Newman, J. D. Dow, and O. F. Sankey, *Appl. Phys. A* **33**, 269 (1987).
- ²⁰R. W. Jansen and O. F. Sankey, *Phys. Rev. B* **36**, 6520 (1987).
- ²¹H. P. Hjalmarson, P. Vogl, D. J. Wolford, and D. J. Dow, *Phys. Rev. Lett.* **44**, 810 (1980).